Pak. J. Bot., 57(5): DOI: http://dx.doi.org/10.30848/PJB2025-5(22)

ECOLOGICAL RESILIENCE MODULATED BY SCLEROMORPHY IN *CAPPARIS DECIDUA* (FORSSK.) EDGEW. POPULATIONS NATIVE TO HYPERARID ENVIRONMENTS

ANUM JAVAID, MANSOOR HAMEED* AND MUHAMMAD SHAHBAZ

Department of Botany, University of Agriculture, Faisalabad 38040, Pakistan
**Corresponding author's hameedmansoor@yahoo.com*

Abstract

Scleromorphy is an adaptive trait, which is crucial to understand survival of bare caper *Capparis decidua* (Forssk.) Edgew. in hyperarid environments. It is a perennial plant with leafless branches and a deep root system that allows it to attain extreme resistance against drought, frost, and salinity. The plant samples (young shoots) were collected from 10 ecologically different habitats from the Cholistan and Thal deserts to evaluate its morpho-anatomy and physiological traits that are associated with its high resistance to hyperarid environment. The Cholistan populations revealed the tallest plants (401.8 cm) with highest shoot dry weight (0.9 g), while populations from the Thal Desert had the thickest cortical region (171.6 µm) and sclerenchyma layer (72.7 µm) which was helpful for conserving more water by storing additional water in storage parenchyma and by minimizing water loss from the stem surface. Vascular bundle (52538.8 μm^2) and metaxylem areas (890.1 µm) were the maximum in the Cholistan populations. Chlorophyll content (1.9 mg g^{-1}) was the highest in Thal populations, while accumulation of organic osmolytes, compatible solutes and antioxidants were the highest in Cholistan populations. It concluded that all population from Thal and Cholistan desert displayed significant variation in its traits that enabled this species to maintain its water status, and hence can withstand hyperarid environmental conditions.

Key words: *Capparis decidua* (Forssk.) Edgew., Ecological success; Plant adaptation; Scleromorphy; Hyperarid environment; Soil-plant relationship.

Introduction

Pakistan's climate and topography make it the most diverse country in the world. Its regions include the plains of the Indus River, the plateaus of Baluchistan and Potohar, the coastal belt, the Baluchistan Basin, the high mountain ranges of the Himalaya, Karakoram, and Hindukush, the Thar and Cholistan deserts, and the Makran coast of Baluchistan (Gadiwala *et al*., 2013). Desert ecosystems are unique in their biodiversity and have their own niches (Quiroga *et al*., 2021). Due to its low organic matter content, desert soil is regarded as poor (Cheema *et al*., 2020). Water is the primary biological component in the desert environment that determines the soil vegetation system (Tesfaye & Negash, 2018). Abiotic stressors that affect desert plants include salinity, dryness, high temperatures, and intense UV radiation. These abiotic factors restrict plant growth and have an impact on morphology and physio-anatomical traits (Rady *et al*., (2016).

To adjust to their surroundings, plants must go through a number of modifications, including the development of wax deposition, stunted growth, deep root system, tiny, scaly leaves, and shorter shoot length (Oliveira *et al*., 2018). Reduced cell area, vascular bundle area, and thicker phloem, mesophyll, and epidermal tissues can all anatomically help to prevent water loss from the surface of plants (Boughalleb *et al*., 2014). Plants can grow continuously because of physiological processes that adapt to their environment; yet abiotic stressors have a significant impact on photosynthetic pigments (Pan *et al*., 2020). To lessen oxidative stress, plants compartmentalize harmful ions, create osmolytes, maintain turgor pressure, water, and ion homeostasis, and control stomatal conductance (Rouphael *et al*., 2017). Stress in the environment hastens the breakdown of chlorophyll, which causes early leaf senescence (Ding *et al*., 2020). Reactive oxygen species produced by stressed plants harm the structure of organelles and other physiological functions (Tripathi *et al*., 2015).

Adaptive strategies based on the existence of structural features, particularly sclerenchyma and parenchyma related to water conservation and mechanical support tissues, are what enable plants to withstand a variety of stresses (De Micco & Aronne, 2012). The finest resource for researching the adaptive components and their mechanisms is natural populations, which have evolved to have high tolerance to abiotic stresses (anatomical modifications in relation to abiotic stresses are summarized in Table 1). To increase crop plant cultivars' tolerance through breeding initiatives, researchers are employing wild plants as models (Palta *et al*., 2012). Hydraulic failure in forest trees, such as *Capparis decidua*, is brought on by trapped gas emboli in the xylary tissue during severe droughts. This might eventually lead to desiccation and even death since it decreases the amount of water available to the leaves for the exchange of photosynthetic gases (Choat *et al*., 2012, 2018).

Growing abundantly in tropical and sub-tropical regions worldwide, *Capparis decidua* (Frossk.) Edgew. is a perennial shrub, woody climber, or small tree that is locally known as karir (Dhakad *et al*., 2016). Around the world, bare caper is extensively found in dry and semi-arid environments (Mir *et al*., 2019). It is a thorny, dense, leafless shrub or tree with caducous leaves, deep roots, grey bark, and red or pink blooms (Dahliya *et al*., 2019). It typically grows in hot, dry, and open environments including wastelands, plains next to slopes, dried ponds, and roadside areas in the Punjab and Sindh desert regions (Kumar *et al*., 2015). In dry, arid environments, it usually demonstrates the CAM pathway as an adaptive response to the surroundings (Patil & Murumkar, 2017). In its natural habitats, bare capers can withstand saline well, according to studies by Sharif & Khan, (2009) and Rafay *et al*., (2022). Up to 40 dS m^{-1} of salt can be tolerated by the bare caper (Vyas *et al*., 2009; Akram *et al*., 2022).

Table 1. Anatomical modifications in plants and their relationship with stress tolerance.

Adaptive components	Relationship with stress tolerance
Epidermis	Thick epidermis minimizes water loss from plant surface (Ahmad *et al*., 2016)
Hypodermis	Hypodermis (sclereid and chlorenchyma) prevents cell collapse and increases photosynthesis capacity (Verma *et al*., 2012)
Parenchyma	Cortical and pith cells (storage parenchyma) are linked to water conservation by storing additional water in prolonged dry environments (Bibi *et al*., 2022)
Sclerenchyma	Sclerification (sclereid cell, stone cell, and cortical fibers) in the outer cortical region, epidermis, and vascular bundles protects delicate calls from collapse (Quintana Pulido *et al*., 2018), minimizes water loss (Ahmad *at al*., 2016)
Vascular tissue	Increased vascular tissue (metaxylem, protoxylem, phloem and sieve areas) is responsible for better transport of water and nutrients as well as photosynthesis (Naz *et al*., 2013), and increases water use efficiency (Ivanova *et al*., 2018)

To investigate the adaptation elements in connection to scleromorphy in bare caper for hyperarid circumstances, we concentrated on the hot, hyperarid deserts in the current study. Plants can withstand extended periods of heat and dryness thanks to a significant phenomenon called scleromorphy, or the hardening of plant organs. The term "sclerophylly" is derived from the Greek words "sklēros" (hard) and "morphs" (a transforming from one shape to another), denoting a hard of plant organs, an adaptation feature of woody plants that aids in their ability to withstand osmotic stress (Alonso-Forn *et al*., 2020). Scleromorphy is primarily caused by lignin deposition in the cortical parenchyma, the epidermis, and particularly in and around vascular tissue (Mansoor *et al*., 2019). It is hypothesized that to withstand the intense heat and aridity of the desert, the variously adapted populations of bare capers may develop flexibility in their morphoanatomical and physiological features as well as in the intensity of their scleromorphy. The following study issues need to be answered: a) Did distinct populations of *C. decidua* differ in terms of scleromorphy? b) Should that be the case, how can scleromorphy aid in the colonization of hyperarid environments?

Materials and Method

Site selection: Populations of *Capparis decidua* were gathered from ten ecologically distinct locations across the Pakistani dry zone in September and October 2021 (Fig. 1). The purpose of the project was to investigate bare caper's adaptive components for hyperarid environments. A quadrat approach was used for soil and plant sampling. One 10-by-10-meter quadrat was drawn out, and it was further divided into 100 1-by-1-meter sub-quadrats. For every sub-quadrat, three plants were randomly selected, and the data were averaged to form one replication (Fig. 2). From each population, three replications were obtained, with a minimum distance of 10 m separating each replication. Nine plants were chosen from every study site. Populations were collected from: Barrage (control): 1) Canal Bank (Dera Ghazi Khan District), Thal Desert: 2) Small Sand Dunes (Mochiwala, Jhang District), 3) Desert Plain (Chobara, Layyah District), and 4) Large Sand Dunes (Mankera, Bhakkar District), and Cholistan Desert: 5) Saline Flat (Derawar Fort, Bahawalpur District), 6) Hypersaline Flat (Lal Sohanra, Bahawalpur District), 7) Desert Flat (Kot Murid. Rhaim Yar Khan District), 8) Fenced Area (Soria Cantonment, Rahim Yar Khan District), 9) Small Sand Dunes (Gaf Bin Tarshom, Rahi Yar Khan District, and 10) Large Sand Dunes (Tuba Nawab Deen, Rahim Yar Khan District). The area near Soria Cantonment was fenced as a hunting ground of Zayed bin Sultan Al Nahyan of the Royal family of United Arab Emirates and totally undisturbed (Table 2).

Soil physicochemical properties: The soil samples near root rhizosphere of each plant (1-2 m deep) were taken with the help of soil auger (diameter 6 cm). Each soil sample was thoroughly mixed and stored in plastic bags, labeled, and brought back to the laboratory for analysis. The 200 g soil sample was oven dried at 105°C and distilled water was added to make saturation paste, which used to test saturation percentage by following formula:

Saturation percentage = Weight of saturation paste–Dry weight of soil

Soil extract was prepared from the saturation percentage, pH and electric conductivity were measured by using pH and ECe meter (WTW series InoLab pH/Cond 720, USA). Soil ionic content (Na^+, Ca^{2+} and K^+) was measured by flame photometer (Jenway, PFP-7) following Toth & Prince (1949). Soil NO_3^- was calculated by micro-Kjeldahl method (Bremner, 1960) using the UDK-132 semiautomatic ammonia distillation unit (NIB-B (3)-DSU-003). Soil PO_4^{3-} was calculated by Wolf (1943) sample dissolved in Bartons reagent and read absorbance at 470 nm using UV-visible spectrophotometer (Hitachi 220, Japan), and value recorded by standard curve (Jackson, 1962).

Environmental data: Data for each ecological site like coordinates and elevation were recorded by GPS (Garmin, eTrex Venture HC, Germany). Meteorological data (maximum and minimum temperature, aridity index and rainfall) were collected from the observatories of Pakistan Meteorological Department positioned at Bhakkar, Noorpur Thal, Khushab, and Jhang (Thal Desert), Bahawal Nagar, Bahawalpur, and Rahim Yar Khan (Cholistan Desert), and Dera Ghazi Khan (http://www.pmd.gov.pk/Observatories/) (Table 2). Budyko-Lettau dryness ratio was calculated by the formula devised by Budyko-Lettau (1969).

$$\text{Dryness ratio} = \frac{R}{P} \times L$$

where R mean annual net radiation (R = 9,855,000 J m^{-2} s^{-1}), P is mean annual precipitation, and L is latent heat of vaporization of water (L = 2260 KJ $mole^{-1}$).

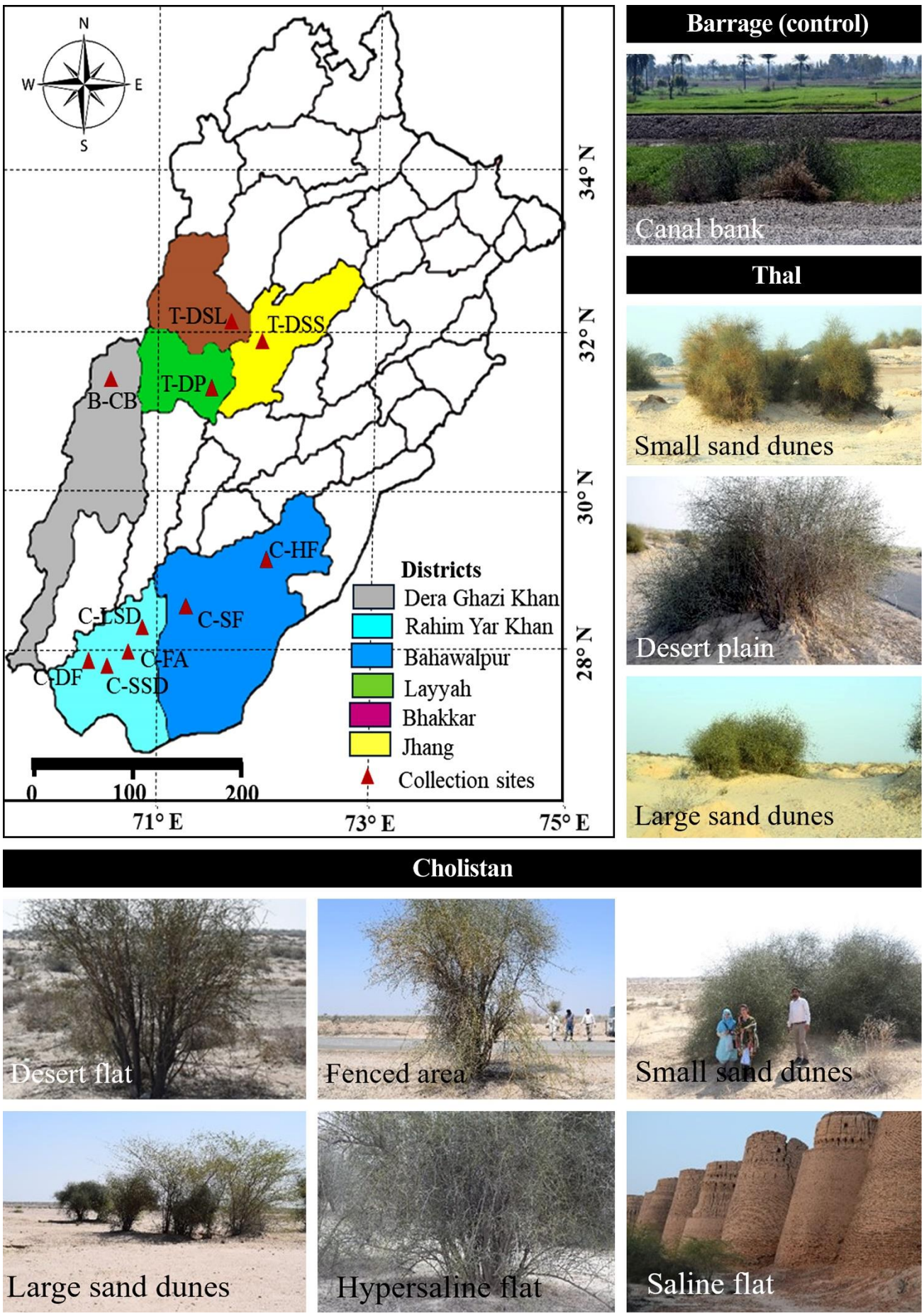

Fig. 1. Map of the Punjab showing collection sites of *Capparis decidua* from hyperarid environments.

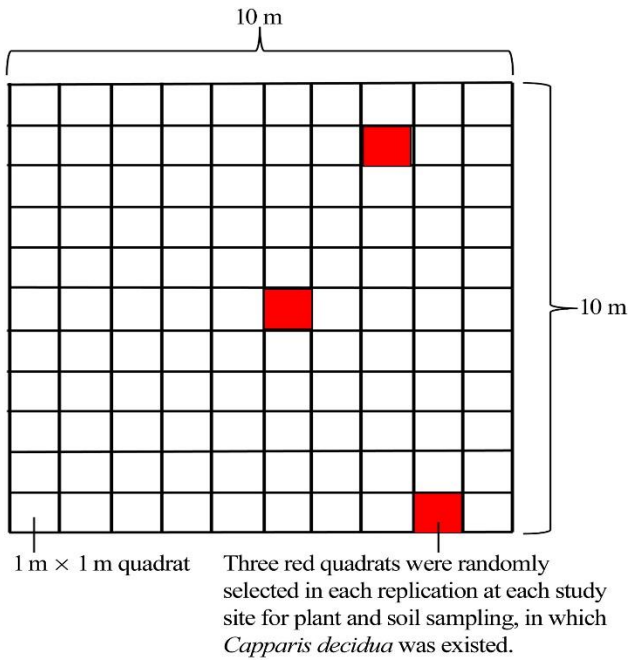

Fig. 2. Soil and plant sampling layout at collection sites of *Capparis decidua* from hyperarid environments.

Morphological characteristics: The plant height was recorded from stem base to the top. Tertiary shoots of last growing season's growth were taken from each plant to calculate the shoot length and fresh weight of those shoots. These shoots were kept in an oven at 65°C until dried completely consistent weight achieved (it took 3 weeks or so), and then recorded dry weights.

Anatomical characteristics: Plant specimen (2 cm long) from the young shoots (between uppermost and second internode) was cut and washed before preserved in formalin acetic alcohol (v/v 5% formalin, 10% acetic acid, 50% ethanol and 35% distilled water) solution for 48 hours. The material was subsequently transferred to acetic alcohol (25% acetic acid, 75% ethanol) solution for anatomical studies. Transverse sections of shoots were prepared by free hand sectioning technique. The thin sections were dehydrated through a serial ethanol grade and stained by safranin and fast green to develop a contrast for microscopic observations following Wang *et al*., (2019). Photographs were taken by camera equipped light microscope (Nikon 104, Japan). Micromorphological data of the prepared sections were recorded by an ocular micrometer that was calibrated with a stage micrometer. Scleromorphy related traits such as intensity of sclerification in epidermis and xylem tissue, and size of cortical fibers, scleride cells, and stone cells were recorded. Other parameters involved in water conservation such as size of storage pith parenchyma and cortical cells, and medullary rays were observed (Fig. 3).

Physiological characteristics

Photosynthetic pigments: Fresh plant material (0.1 g) was ground into 5 ml of 80% acetone and centrifuged. Extract was used to measure the chlorophyll *a*, *b* and carotenoids by UV-Visible spectrophotometer (Hitachi 220, Japan) following Arnon (1949) protocol.

Antioxidants: Plant material 0.5 g was ground in 5 mL potassium phosphate buffer and the extract was filtered after centrifugation to determine the antioxidant activity in the plant. UV-visible spectrophotometer (Hitachi 220, Japan) used for the estimation of antioxidants in plants. The antioxidant superoxide dismutase activity was estimated (400 µL distilled water + 250 µL phosphate buffer + 100 µL methionine + 100 µL triton + 50 µL solution of NBT (nitroblue tetrazolium + enzyme extract and 50 µL riboflavin) added together and placed under illuminated fluorescent light for 20 min and read at 560 nm (Giannopolitis & Ries, 1977).

The Chance & Maehly (1955) method were followed for catalase assay (1.9 mL potassium phosphate buffer + 100 µL hydrogen per oxide + 100 µL enzyme extract mixed and read at 560 nm with time interval of 0 sec., 30 sec. and 60 sec. In contrast, peroxidase was estimated by adding 750 µL phosphate buffer, 100 µL giochol, 100 µL H_2O_2 and enzyme extract together in a tube and read absorbance at 470 nm after 30 seconds (Onsa *et al*., 2004). To determine the malondialdehyde, plant material (0.25 g) was chopped in 250 µL tricarboxylic acid and thiobarbituric acid in test tubes, boiled in water bath for 30 min., cooled with ice water, diluted the mixture up to 1mL and centrifuged to obtain supernatant. The absorbance was read at 532 and 600 nm (Heath & Packer, 1968).

For the estimation of non-enzymatic H_2O_2 (0.25 g of material crushed in 5 ml tricarboxylic acid and centrifuged. The 500 µL supernatant, 500 µL phosphate buffer, and 1 ml potassium iodide were mixed in test tubes, vortexed for 1 min and absorbance was recorded at 390 nm (Velikova *et al*., 2000). For ascorbic acid, 0.1 g plant material was ground in 5 mL trichloroacetic acid (6%) and centrifuged. Then in each tube, 1 mL extract, 1 mL of 2% dinitrophenyl hydrazine, and 1 drop of 10% thiourea were added, boiled in water bath for 15 min, cooled by using ice and 5 ml 80% H_2SO_4 was added and stored at 0°C. The mixture was read at 530 nm and reading was compared with standard curve to obtain original concentration of ascorbic acid (Mukherjee & Choudhuri, 1983).

***Organic osmotica*:** For total amino acids, extract was obtained by 1 g crushed in 10 mL citrate buffer, incubate for one hour at 25°C, centrifuged and supernatant discarded. Then added 1 mL of ninhydrin solution to 1 ml of extract, covered with aluminum foil, boiled in water bath for 20 min., cooled with cold water, diluted up to 5 mL by distilled water, mixed well and again incubated for 15 min. The absorbance was read at 570 nm and reading was compared with leucine standard curve (Moore & Stein, 1948).

For soluble sugars, 0.1 g of material grinded in 80% ethanol solution and extract was incubated at 60°C for six hours. Thereafter 300 µL anthrone reagent was added in 100 µL extract, heated in water bath for 10 min. cooled with ice for ten min, and incubated at room temperature for 20 min. The absorbance was read at 625 nm and calculated the exact concentration of total soluble sugar by using the standard curve (Yemm & Willis, 1954).

For total soluble proteins, 0.5 g of plant material was crushed in 5 mL potassium phosphate buffer and centrifuged to obtain extract. Bradford dye was prepared by using standard protocol (G250 Commasie brilliant blue). One mL dye was added to 5 µL enzyme extract, the reading was taken at 595 nm and calculated value was compared with standard curve that developed by using of Bovine serum albumin to compute the original value (Bradford, 1976).

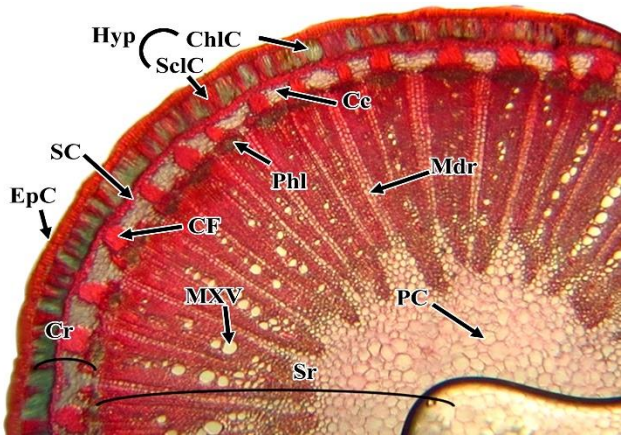

Fig. 3. Stem transverse indicating measurement of different tissues and cells *Capparis decidua.*
EpC- Epidermis cell, Cr- Cortical region, Hyp- Hypodermis layer, SclC- Sclereid cell, SC- Stone cell, ChlC- Chlorenchyma cells, Cc- Cortical cells, CF- Cortical fibres, Phl- Phloem cells, Mdr- Medullary rays, MXV- Metaxylem vessels, PC- Pith cells, Sr- Steller region

To estimate the proline, 0.1 g of plant material was chopped in 10 mL of 3% sulfo-salicylic acid and centrifuged to obtain extract. One mL extract was taken and added 1 mL acid ninhydrin solution and 1 mL of glacial acetic acid in each test tube and heated for 1 h at 100°C. It was then cooled by ice bath and added 4 mL toluene and shake vigorously. After some time, two distinct layers were clearly formed in tubes and the upper layer used to read absorbance at 520 nm. The reading was compared with standard curve to obtain original concentration of proline (Bates *et al*., 1973).

To determine glycine betaine, 0.25 g was crushed in 5 ml distilled water, centrifuged to obtain extract. The extract was diluted with 2N H_2SO_4. The diluted extract (0.5 mL) was placed in ice for one hour, then added 0.2 mL IK-I_2 reagent, 2.8 mL distilled water, and 6 mL 1, 2-dichloroethane. The reaction ended by forming two layers. The lower layer was taken, and absorbance was read at 365 nm. The estimated value compared with standard curve to compute the original value (Grieve & Grattan, 1983).

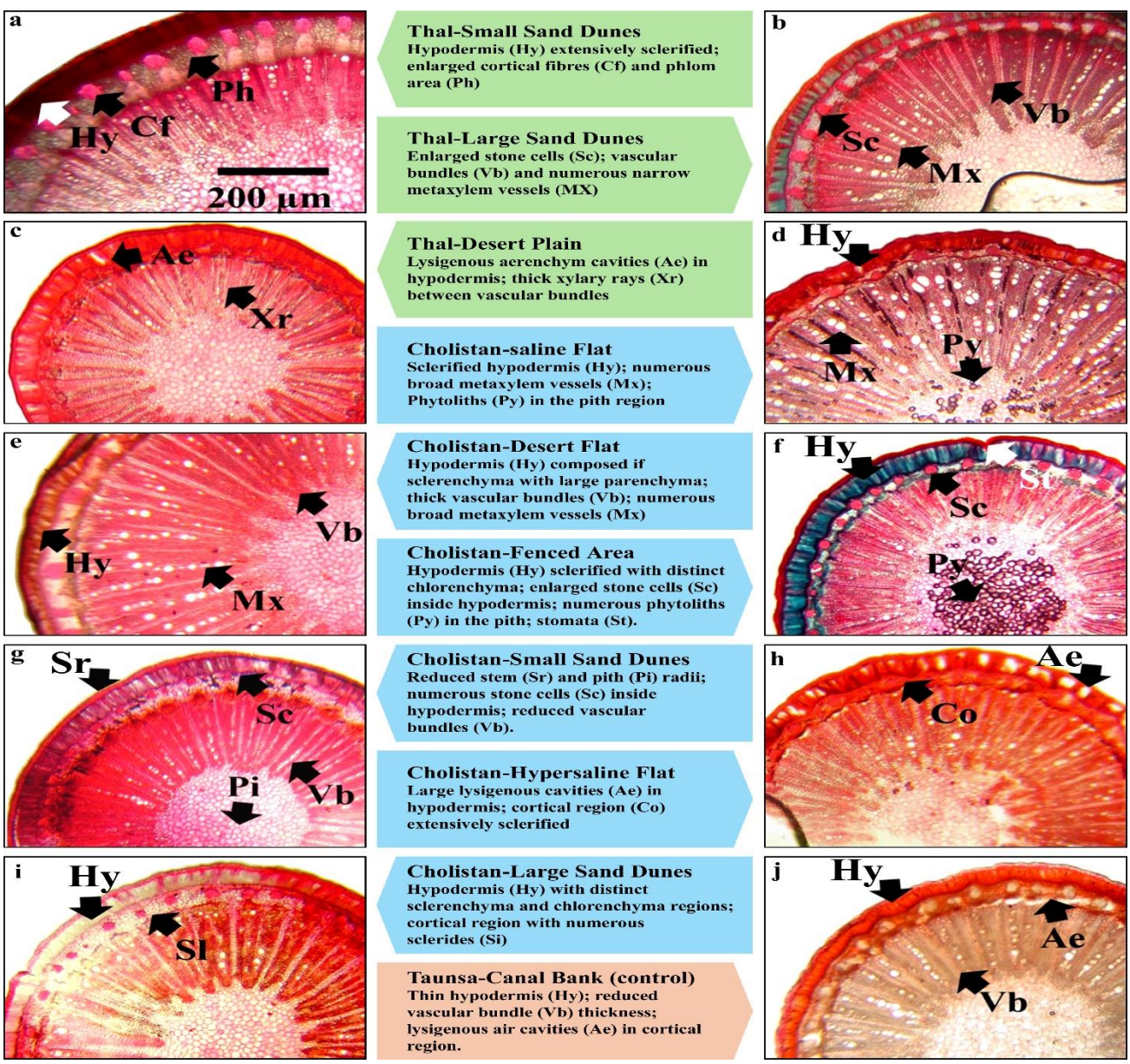

Fig. 4. Stem transverse sections of *Capparis decidua* collected from different hyperarid environments.

Table 2. Collection sites and habitat description *Capparis decidua* populations collected from hyperarid desert habitats.

Region	Districts	Site collection	Habitat	Land used	Rainfall (mm)	Temperature (°C)		Dryness ratio	Coordinates	Elevation (m a.s.l.)
						Max	Min			
Thal Desert	Jhang	Mochiwala	Thal-Small Sand Dunes	Chickpea cultivation	263.2	40	6	16.6	31°19'38.24"N 72°01'29.90"E	166
	Layyah	Chubara	Thal-Desert Plain	Livestock grazing, chickpea cultivation	185.3	41	7	23.6	30°53'42.94"N 71°29'55.46"E	144
	Bhakkar	Mankera	Thal-Large Sand Dunes	Chickpea cultivation and citrus cultivation through drip irrigation.	234.6	40	6	18.6	31°23'53.48"N 71°26'11.54"E	159
Cholistan Desert	Bahawalpur	Derawar Fort	Cholistan-Saline Flat	Heavy livestock grazing pressure	130.1	41	7	33.5	28°45'68.62"N 71°19'58.48"E	109
		Lal Sohanra	Cholistan-Hypersaline Flat	Undisturbed area	156.9	40	7	27.8	29°29'47.42"N 72°05'42.48"E	131
	Rahim Yar Khan	Kot Murid	Cholistan-Desert Flat	Low livestock grazing pressure	98.6	42	8	44.2	28°22'59.51"N 70°45'51.30"E	89
		Soria Cantonment	Cholistan-Fenced Area	Undisturbed natural desert habitat	101.7	43	8	42.9	28°18'53.99"N 70°37'24.92"E	87
		Gaf Bin Tarshom	Cholistan-Small Sand Dunes	Low livestock grazing pressure	103.3	42	8	42.2	28°17'52.74"N 70°28'27.50"E	91
		Toba Nawab Deen	Cholistan-Large Sand Dunes	High livestock grazing pressure	97.8	43	8	44.6	28°36'17.34"N 71°06'07.46"E	96
Barrage	Dera Ghazi Khan	Taunsa Barrage	Barrage-Canal Bank (control)	Cultivation of cereals, fodder, and forage species	149.9	42	9	29.1	30°31'21.59"N 70°50'27.13"E	135

According to UNESCO (1979) classification, all sites were hyperarid

Table 3. Soil physicochemical traits of *Capparis decidua* populations collected from hyperarid desert habitats.

Traits	Collection sites									
	T-DSS	T-DP	T-DSL	C-SF	C-HF	C-DF	C-FA	C-SSD	C-LSD	B-CB
Soil moisture regimes*	Aridic	Aridic	Aridic	Aridic	Aridic	Aridic	Aridic	Aridic	Aridic	Ustic
USDA soil classification based on soil texture class	Loamy sand	Sandy loam	Sand	Sandy loam	Sandy loam	Loamy sand	Loamy sand	Loamy sand	Sand	Loam
Saturation percentage (%)	17 ± 0.9de	22 ± 0.7bc	14 ± 0.9d	21 ± 0.9bc	24 ± 0.5b	24 ± 0.7b	20 ± 0.9cd	16 ± 0.5ef	13 ± 0.5f	32 ± 0.9a
pH	8.2 ± 0.2bc	8.3 ± 0.3abc	8.1 ± 0.2c	8.4 ± 0.2ab	8.3 ± 0.4abc	8.3 ± 0.2abc	8.4 ± 0.4ab	8.5 ± 0.3a	8.5 ± 0.2a	7.7 ± 0.2d
ECe (dS m^{-1})	1.9 ± 0.3d	0.9 ± 0.2d	4.8 ± 0.2c	14.7 ± 0.3b	25.3 ± 0.2a	1.6 ± 0.2d	2.4 ± 0.4d	1.4 ± 0.3d	1.9 ± 0.2d	1.5 ± 0.4d
Na^{+} (mg kg^{-1})	174.8 ± 0.5ef	139.7 ± 0.4f	429.2 ± 0.4c	2518.3 ± 0.4b	3439.9 ± 0.3a	184.3 ± 0.4e	298.5 ± 0.5d	218.3 ± 0.3e	214.5 ± 0.5e	196.9 ± 0.3e
Ca^{2+} (mg kg^{-1})	56.4 ± 0.6cd	57.2 ± 0.5c	71.18 ± 0.5b	54.5 ± 0.6c	56.6 ± 0.6c	55.2 ± 0.4c	64.9 ± 0.4bc	72.4 ± 0.5b	37.6 ± 0.6d	89.3 ± 0.4a
K^{+} (mg kg^{-1})	127.9 ± 0.4b	75.7 ± 0.4e	106.4 ± 0.5cd	76.8 ± 0.4e	61.6 ± 0.3f	69.3 ± 0.4ef	112.8 ± 0.5c	98.6 ± 0.5d	59.4 ± 0.4f	149.7 ± 0.5a
PO_4^{3-} (mg kg^{-1}),	2.7 ± 0.4d	9.1 ± 0.3b	3.7 ± 0.3cd	9.6 ± 0.4b	4.4 ± 0.4cd	5.4 ± 0.3c	7.9 ± 0.3b	8.2 ± 0.4b	11.9 ± 0.3a	8.8 ± 0.4b
NO_3^{-} (mg kg^{-1})	0.1 ± 0.3fg	8.5 ± 0.4a	0.04 ± 0.3g	2.8 ± 0.3cde	2.4 ± 0.4de	2.9 ± 0.4cde	3.8 ± 0.3bc	4.8 ± 0.4b	4.2 ± 0.3b	1.9 ± 0.3ef

*USDA Soil Taxonomy

Letters sharing similar letters are statistically not significant at $p<0.05$

Collection sites: T-DSS (Thal Desert small sand dunes), T-DP (Thal Desert plain), T-DSL (Thal Desert large sand dunes), C-SF (Cholistan Desert saline flat), C-HF (Cholistan Desert hypersaline flat), C-DF (Cholistan Desert flat), C-FA (Cholistan Desert fenced area), C-SSD (Cholistan Desert small sand dunes), C-LSD (Cholistan Desert large sand dunes), B-CB (Along canal bank-moist habitat)

To calculate the phenolic compound and flavonoid extract was obtained by 0.1 g material ground in 5 ml of acetone (80%) and centrifuged. For phenolic compounds, 100 µL extract, 1 mL distilled water, 0.5 mL Folin-Ciocalteu phenol reagent were added in test tubes, shake vigorously, and added 2.5 ml 20% Na_2CO_3. The mixture was then vortexed, and reading was noted at 750 nm (Julkenun-Titto, 1985). For flavonoids, 1 mL extract diluted up to 5 ml by distilled water, and the added 0.6 mL of 5% $NaNO_3$, 0.5 mL 10% Al_2Cl_3, 2.5 mL 1N NaOH, and 2.4 mL distilled H_2O, and mixed thoroughly. The absorbance was noted at 510 nm (Zhishen *et al*., 1999).

Statistical analysis

The data were statistically analyzed Microsoft Excel for analysis of variance in completely randomized design with three replications. The means were compared with the Least Significant Difference Test. The data were also put to multivariate principal component analysis (PCA) using XLSTAT (ver 2021.1.) to evaluate the association between different physicochemical properties with morpho-anatomical and physiological traits of bare caper.

Results

Soil physicochemical properties: The population collected from large sand dunes of Cholistan revealed the lowest saturation percentage (13%), soil Ca^{2+} (37.6 mg kg^{-1}) and K^+ (59.4 mg kg^{-1}), and the highest soil pH (8.5) and PO_4^{3-} (11.9 mg kg^{-1}) (Table 3). The population from moist habitat canal bank showed the highest saturation percentage (32%), soil Ca^{2+} (89.3 mg kg^{-1}) and K^+ (309.7 mg kg^{-1}), and the lowest soil pH (7.7). The population from Cholistan-hypersaline flat displayed the highest ECe (25.3 dS m^{-1}) and Na^+ (3439.9 mg kg^{-1}), while the population from Cholistan-small sand dunes revealed the highest pH (8.5) (Table 3). The population from Thal-desert plain possessed the lowest Na^+ (139.7 mg kg^{-1}), soil ECe (0.9 dS m^{-1}), and the highest NO^{3-} (8.5 mg kg^{-1}). The population from Thal-small sand dunes revealed the lowest PO_4^{3-} (2.7 mg kg^{-1}), and that from Thal-large sand dunes had the lowest NO^{3-} (0.04 mg kg^{-1}) (Table 3).

Morphological traits: The population from Cholistan-large sand dunes showed the tallest plants (401.8 cm), while the smallest plants (198.5 cm) were observed in the population from canal bank moist habitat. The population from small sand dunes of Cholistan displayed the longest shoots (28.3 cm), while the shortest shoots (13.8 cm) were seen in the desert plain population of Thal (Table 4). The populations from saline flat, desert flat and hypersaline flat from the Cholistan showed the highest dry weight (0.9 g), whereas hypersaline flat population of Cholistan exhibited the highest fresh weight (9.1 g). The desert plain population of Thal revealed the lowest dry (0.3 g) and fresh weight (2.9 g) (Table 4).

Anatomical traits: The large sand dunes population of Cholistan exhibited the thickest epidermis (25.3 µm), and thinnest hypodermis (40.1 µm). The small sand dunes population of Thal revealed the highest stem radius (1119.3 µm), hypodermis thickness (69.5 µm), cortical region thickness (171.6 µm), sclereid thickness (72.2 µm), stone cells thickness (24.5 µm), phloem thickness (87.9 µm), pith cell thickness (441.2 µm), pith cell area (1270.9 μm^2), and stelar region thickness (844.2 µm). The population from saline flats of Cholistan showed the largest cortical cells (290.2 μm^2), while the hypersaline flat population of Cholistan had the highest vascular bundle thickness (514.7 µm) (Table 4, Fig. 4).

The large sand dunes population of Thal displayed the lowest stone cells thickness (13.6 µm), and phloem thickness (26.9 µm). The Thal-desert plain population had the lowest cortical cell area (58.8 μm^2), cortical fibers thickness (437.8 µm), while small sand dunes population of Cholistan had the narrowest metaxylem vessels (229.3 μm^2) (Table 4, Fig. 4). and the canal bank moist habitat population showed the lowest stone cells thickness (32.7 µm). The desert flat population of Cholistan revealed the highest cortical fibers thickness (2199. µm), metaxylem area (890.1 μm^2), and vascular bundle area (52538.8 μm^2), and the lowest epidermis thickness (16.3 µm) (Table 4, Fig. 4).

The fenced area population of Cholistan presented the lowest stem radius (482.1 µm), cortical thickness (81.7 µm), stone cells thickness (13.1 µm), phloem thickness (26.6 µm), pith thickness (106.2 µm), vascular bundle thickness (250.6 µm), pith area (209.8 μm^2), vascular bundle area (8041.7 μm^2), and stelar region thickness (356.8 µm) (Table 4, Fig. 4).

Physiological traits: The large sand dunes population of Thal showed the highest Chlorophyll *a* (1.9 mg g^{-1} fresh weight), and the lowest glycine betaine (0.63 µm g^{-1}), and hydrogen peroxide (32.3 µm g^{-1}). The desert flat population of Cholistan revealed the lowest chlorophyll *b* (0.13 mg g^{-1} fresh weight), carotenoids (0.002 mg g^{-1} fresh weight), and ascorbic acid (11.09 µg ml^{-1}), whereas the highest hydrogen peroxides (40.3 µm g^{-1}), was recorded in this population (Table 5). The population from large sand dunes of Cholistan showed the lowest chlorophyll *a* (1.08 mg g^{-1} fresh weight), and the highest chlorophyll *b* (0.52 mg g^{-1} fresh weight), soluble sugar (8.5 µg g^{-1}), proline (38.6 µm g^{-1}), phenolic compounds (49.7 µg g^{-1} fresh weight), malondialdehyde enzyme (6.7 nmol g^{-1}), and peroxidase (0.11 Units μg^{-1} protein) (Table 5).

The population from saline flat of Cholistan showed the highest carotenoids (0.010 mg g^{-1} fresh weight), and lowest soluble sugars (3.3 µg g^{-1}), flavonoids (0.7 µg g^{-1} fresh weight), phenolic compounds (11.5µg g^{-1} fresh weight), peroxidase (0.03 Units μg^{-1} protein), and catalase (0.05 Units mg^{-1} protein). The desert plain population of Thal showed highest soluble proteins (1918.4 µg g^{-1}), and the lowest superoxide dismutase activity (0.03 Units mg^{-1} protein). The fenced area population of Cholistan displayed lowest soluble proteins (833.4 µg g^{-1}), and the highest superoxide dismutase (6.09 Units mg^{-1} protein), and catalase activity (0.17 Units mg^{-1} protein) (Table 5).

The small sand dunes population of Cholistan showed the highest free amino acids (18.7 µg g^{-1}), and the canal bank moist habitat population revealed the highest glycine betaine (3.5 µm g^{-1}), and lowest malondialdehyde activity (1.2 nmol g^{-1}). The hypersaline flat population of Cholistan showed lowest free amino acid (7.1 µg g^{-1}), proline (18.6 µmol g^{-1}), and peroxidase activity (0.03 Units μg^{-1} protein), and highest ascorbic acid (54.8 µg ml^{-1}), and flavonoids (1.7 µg g^{-1} fresh weight) (Table 5).

Table 4. Plant morphological and stem anatomical traits of *Capparis decidua* populations collected from hyperarid desert habitats.

Traits	Collection sites									
	T-DSS	T-DP	T-DSL	C-SF	C-HF	C-DF	C-FA	C-SSD	C-LSD	B-CB
	Morphology									
Plant height (cm)	246.6 ± 0.2de	258.7 ± 0.3d	240.6 ± 0.3de	203.7 ± 0.3f	231.5 ± 0.2e	283.5 ± 0.2c	350.5 ± 0.2b	296.2 ± 0.4c	401.8 ± 0.3a	198.5 ± 0.2f
Shoot length (cm)	21.6 ± 1c	13.8 ± 0.5e	19.6 ± 0.5c	14.9 ± 0.7de	16.3 ± 0.5d	27.3 ± 1ab	27.9 ± 1a	28.3 ± 0.5a	16.6 ± 1d	25.4 ± 1b
Shoot fresh weight (g)	8.3 ± 0.08a	2.9 ± 0.4d	6.4 ± 0.1b	8.5 ± 0.1a	9.1 ± 0.1a	8.8 ± 0.1a	5.8 ± 0.2b	3.6 ± 0.2cd	4.1 ± 0.1c	5.8 ± 0.2b
Shoot dry weight (g)	0.8 ± 0.01a	0.3 ± 0.04d	0.6 ± 0.01b	0.9 ± 0.01a	0.9 ± 0.03a	0.9 ± 0.02a	0.6 ± 0.02b	0.4 ± 0.02cd	0.4 ± 0.01cd	0.6 ± 0.01b
	Stem Anatomy									
Stem radius (μm^2)	1119.3 ± 3a	522.9 ± 4f	776.2 ± 4d	654.4 ± 4e	996.7 ± 4b	923.2 ± 4c	482.1 ± 4g	604.6 ± 4ef	751.6 ± 4d	759.8 ± 4d
Epidermal thickness (μm)	16.4 ± 0.9b	16.4 ± 0.4b	23.6 ± 0.4a	24.5 ± 0.4a	16.4 ± 0.4b	16.3 ± 0.4c	23.7 ± 0.4a	16.4 ± 1b	25.3 ± 1a	24.5 ± 0.4a
Hypodermis thickness (μm)	69.5 ± 2.3a	49.8 ± 0.4b	49.2 ± 0.4c	53.1 ± 2.3bc	61.5 ± 2.6ab	49.1 ± 1.4c	51.5 ± 2.8bc	55.6 ± 1.8bc	40.1 ± 0.4c	44.9 ± 2.3cd
Cortical region thickness (μm)	171.6 ± 4a	114.4 ± 0.9cd	99.4 ± 1d	134.8 ± 2.3b	95.9 ± 1.6de	98.1 ± 1.4d	81.7 ± 4e	118.5 ± 2.3c	114.4 ± 4cd	112.8 ± 0.9cd
Cortical cell area (μm^2)	105.2 ± 1.5d	58.8 ± 3e	106.6 ± 1d	290.2 ± 2.4a	87.9 ± 3.4e	60.3 ± 1.4e	60.8 ± 2e	110.4 ± 1.8d	157.6 ± 3.6c	206.6 ± 2.5b
Cortical fibres area (μm^2)	1838.5 ± 1.6bc	437.8 ± 1.5g	1270.9 ± 2.3d	1037.9 ± 1.5ef	1896.7 ± 2b	2199.1±2.4a	520.3 ± 2.1fg	542.3 ± 2.7f	1533.6 ± 1.4cd	1563.9 ± 1.5c
Sclereid thickness (μm)	72.7 ± 0.9	57.2 ± 0.4	46.6 ± 1.6	55.6 ± 0.9	57.2 ± 0.9	36.8 ± 0.9	41.7 ± 0.4	36.7 ± 0.4	36.7 ± 1	32.7 ± 0.4
Stone cell area (μm)	24.5 ± 0.4a	8.9 ± 0.9g	13.6 ± 1.4e	17.9 ± 0.9bc	14.7 ± 0.9d	16.3 ± 2.3c	13.1 ± 0.4ef	14.7 ± 2.3d	14.2 ± 2.3de	15.5 ± 1.4c
Phloem Thickness (μm)	87.9 ± 3a	33.5 ± 0.9de	26.9 ± 1.4de	36.7 ± 2.3d	44.9 ± 2.3cd	38.1 ± 1.6d	26.6 ± 1.8e	51.5 ± 0.4b	46.8 ± 1.4c	46.3 ± 1.6c
Pith thickness (μm)	441.2 ± 1.3a	198.8 ± 2.7de	354.1 ± 3.2b	209.7 ± 2.3d	299.6 ± 4.7bc	250.6 ± 2.3cd	106.2 ± 3.3f	187.9 ± 2.3e	266.9 ± 4.8c	250.6 ± 2.4cd
Vascular bundle thickness (μm)	403.5 ± 1.9b	264.2 ± 4.7e	299.7 ± 2.1d	326.8 ± 4.7cd	514.7 ± 2.5a	503.8 ± 2.3a	250.6 ± 1.4e	315.9 ± 4.7cd	305.1 ± 3.6d	343.2 ± 4.7c
Metaxylem area (μm^2)	653.5 ± 1.5b	247.4 ± 2.1e	655.5 ± 2.5b	490.4 ± 1.2cd	488.2 ± 2.1d	890.1 ± 1.3a	238.4 ± 3.6e	229.3 ± 1.7e	517.3 ± 1.5cd	665.4 ± 3.4b
Pith cell area (μm^2)	1270.9 ± 1.7a	484.6 ± 1de	594.4 ± 2.6cd	626.3 ± 1.6c	315.5 ± 0.4ef	640.1 ± 2c	209.8 ± 0.6f	633.5 ± 3.2c	832.1 ± 3.4b	773.1 ± 3.5bc
Vascular bundle area (μm^2)	25803.2 ± 2.9cd	15349.7 ± 1.5de	12097.4 ± 3e	15366.6 ± 2.8de	21458.9 ± 2.8d	52538.8 ± 4a	8041.7 ± 3.2f	17446.9 ± 3.7de	32673.6 ± 1.9c	43444.6 ± 3.1ab
Stelar region thickness (μm)	844.2 ± 3a	462.9 ± 2.8f	653.6 ± 2.7c	536.5 ± 1.6e	814.3 ± 2.8ab	754.4 ± 3b	356.8 ± 2.2g	503.8 ± 3.1e	571.9 ± 1.1d	593.7 ± 1.8d

Letters sharing similar letters are statisticall not significant at $p<0.05$

Collection sites: T-DSS (Thal Desert small sand dunes), T-DP (Thal Desert plain), T-DSL (Thal Desert large sand dunes), C-SF (Cholistan Desert saline flat), C-HF (Cholistan Desert hypersaline flat), C-DF (Cholistan Desert flat), C-FA (Cholistan Desert fenced area), C-SSD (Cholistan Desert small sand dunes), C-LSD (Cholistan Desert large sand dunes), B-CB (Along canal bank-moist habitat)

Table 5. Plant physiological traits of *Capparis decidua* populations collected from hyperarid desert habitats.

Traits	Collection sites									
	Thal			Cholistan						Control
	Small sand dunes	Desert plain	Large sand dunes	Saline flat	Hypersaline flat	Desert flat	Fenced area	Small sand dunes	Large sand dunes	Canal bank
Chlorophyll *a* (mg g^{-1} fresh weight)	1.9 ± 0.01a	1.8 ± 0.01ab	1.8 ± 0.01ab	1.3 ± 0.02bc	1.1 ± 0.01d	1.5 ± 0.01b	1.4 ± 0.02b	1.3 ± 0.01bc	1.0 ± 0.01d	1.3 ± 0.02bc
Chlorophyll *b* (mg g^{-1} fresh weight)	0.37 ± 0.02bc	0.32 ± 0.01c	0.31 ± 0.02c	0.14 ± 0.01ef	0.49 ± 0.01a	0.13 ± 0.01ef	0.29 ± 0.01d	0.26 ± 0.03d	0.52 ± 0.01a	0.22 ± 0.01de
Carotenoids (mg g^{-1} fresh weight)	0.04 ± 0.001cd	0.03 ± 0.001d	0.03 ± 0.001d	0.10 ± 0.001a	0.07 ± 0.001b	0.02 ± 0.001e	0.03 ± 0.001d	0.02 ± 0.001e	0.07 ± 0.001b	0.05 ± 0.001c
Total soluble proteins (µg g^{-1})	884.7 ± 0.7e	1918.4 ± 0.7a	1482.6 ± 0.7b	1465.5 ± 0.7b	973.1 ± 0.7d	842.6 ± 0.7e	833.4 ± 0.7e	880.8 ± 0.7e	933.5 ± 0.7d	1341.7 ± 0.7c
Total soluble sugar (µg g^{-1})	5.1 ± 0.02d	3.7 ± 0.02f	4.4 ± 0.02e	3.3 ± 0.02g	6.3 ± 0.02c	5.4 ± 0.02d	3.7 ± 0.02f	5.8 ± 0.02c	8.5 ± 0.02a	6.6 ± 0.02b
Free amino acid (µg g^{-1})	10.5 ± 0.07bc	7.9 ± 0.07cd	9.2 ± 0.07c	9.8 ± 0.07bc	7.1 ± 0.07d	10.8 ± 0.07b	8.3 ± 0.07cd	18.7 ± 0.07a	8.9 ± 0.07c	10.7 ± 0.07bc
Glycine betaine (µmol g^{-1})	0.63 ± 0.2d	2.5 ± 0.2b	1.5 ± 0.2cd	1.7 ± 0.1c	0.61 ± 0.1d	1.8 ± 0.2c	3.3 ± 0.2a	2.2 ± 0.2bc	1.6 ± 0.2c	3.5 ± 0.2a
Proline (µmol g^{-1})	23.6 ± 0.3cd	20.8 ± 0.2de	25.6 ± 0.3c	31.8 ± 0.6b	18.6 ± 0.3e	24.5 ± 0.1c	18.6 ± 0.3e	20.6 ± 0.5de	38.6 ± 0.5a	22.3 ± 0.1d
Ascorbic acid (µg ml^{-1})	21.2 ± 0.7d	20.6 ± 0.6d	25.9 ± 0.3c	14.1 ± 0.4de	54.8 ± 0.3a	11.09 ± 0.4e	28.1 ± 0.3c	46.4 ± 0.4b	14.7 ± 0.4de	13.1 ± 0.6de
Hydrogen peroxide (µmol g^{-1})	32.3 ± 0.8	38.2 ± 0.2	39.1 ± 0.2	37.9 ± 0.2	40.1 ± 0.2	40.3 ± 0.2	38.7 ± 0.1	37.03 ± 0.2	34.7 ± 0.1	34.8 ± 0.1
Flavonoids (µg g^{-1} fresh weight)	1.19 ± 0.02b	0.76 ± 0.02c	1.1 ± 0.01b	0.70 ± 0.04c	1.71 ± 0.01a	0.8 ± 0.01c	0.75 ± 0.01c	0.99 ± 0.01bc	1.10 ± 0.01b	1.04 ± 0.02bc
Phenolics (µg g^{-1} fresh weight)	45.9 ± 1.5a	19.1 ± 0.9f	32.9 ± 1d	11.5 ± 0.4g	23.4 ± 0.7f	33.4 ± 0.5d	26.4 ± 1.6e	35.7 ± 0.6c	49.7 ± 2.5a	43.4 ± 0.7b
Malondialdehyde (nmol g^{-1})	6.2 ± 0.1ab	1.8 ± 0.1e	6.05± 0.2ab	1.3 ± 0.1e	1.3 ± 0.2e	2.9 ± 0.1d	6.9 ± 0.1a	3.4 ± 0.1c	6.7 ± 0.1a	1.2 ± 0.1e
Peroxidase (Units mg^{-1} protein)	0.5 ± 0.03bc	0.4 ± 0.01c	0.6 ± 0.02b	0.3 ± 0.01cd	0.3 ± 0.04cd	0.8 ± 0.01b	0.3 ± 0.03	0.5 ± 0.01bc	1.1 ± 0.02a	0.7 ± 0.01b
Superoxide dismutase (Units mg^{-1} protein)	5.2 ± 0.05a	0.03 ± 0.02e	4.1 ± 0.05b	5.5 ± 0.05a	3.8 ± 0.06c	3.7 ± 0.04c	6.09 ± 0.04a	5.6 ± 0.05a	1.3 ± 0.05d	1.4 ± 0.01d
Catalase (Units mg^{-1} protein)	1.4 ± 0.1b	1.2 ± 0.1bc	1.5 ± 0.1ab	0.5 ± 0.06d	1.1 ± 0.03c	0.6 ± 0.01d	1.7 ± 0.1a	1.2 ± 0.1bc	0.7 ± 0.04d	1.0 ± 0.05cd

Letters sharing similar letters are statistically not significant at $p<0.05$

Collection sites: T-DSS (Thal Desert small sand dunes), T-DP (Thal Desert plain), T-DSL (Thal Desert large sand dunes), C-SF (Cholistan Desert saline flat), C-HF (Cholistan Desert hypersaline flat), C-DF (Cholistan Desert flat), C-FA (Cholistan Desert fenced area), C-SSD (Cholistan Desert small sand dunes), C-LSD (Cholistan Desert large sand dunes), B-CB (Along canal bank-moist habitat)

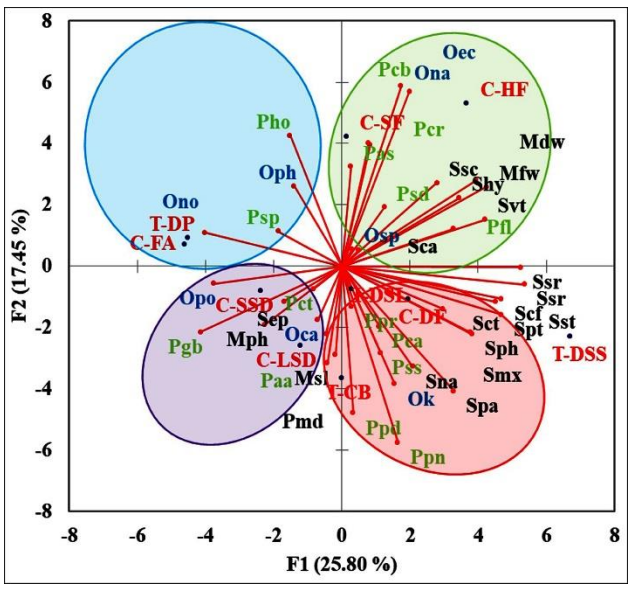

Fig. 5. Relationship among soil physicochemical traits and plant morpho-anatomical and physiological traits of *Capparis decidua* collected from different hyperarid environments

Site collections: T-DSS Thal Desert small sand dunes, T-DP Thal Desert plain, T-DSL Thal Desert large sand dunes, C-SF Cholistan Desert saline flat, C-HF Cholistan Desert hypersaline flat, C-DF Cholistan Desert flat, C-FA Cholistan Desert fenced area, C-SSD Cholistan Desert small sand dunes, C-LSD Cholistan Desert large sand dunes, T-CB Along canal bank (moist habitat).

Morphological traits: Mph-Plant height, Msl-Shoot length, Mfw-Shoot fresh weight, Mdw-Shoot dry weight.

Physiological traits: Pca-Chlorophyll a, Pcb-Chlorophyll b, Pcr-Carotenoids, Ppr-Proline, Pgb-Glycine betaine, Psp-Total soluble proteins, Pss-Total soluble protein, Paa-Free amino acid, Psd-Superoxide dismutase, Pmd-Malondialdehyde, Pct-Catalase, Ppd-Peroxidase. Pas-Ascorbic acid, Pfl-Flavonoids, Ppn-Phenolic compounds, Pho-Hydrogen peroxide.

Anatomical traits: Sep-Epidermal thickness, Shy-Hypodermis thickness, Sct-Cortical region thickness, Sca-Cortical cell area, Ssc-Sclereid thickness, Sst-Stone cell area, Sva-Vascular bundle area, Smx-Metaxylem area, Sph-Phloem Thickness; Spt-Pith thickness, Spa-Pith cell area. Svt-Vascular bundle thickness, Scf-Cortical fibres area, Ssr-Stelar region thickness, Srd-stem radius.

Soil traits: Oca-soil Ca^{2+}, Ok-soil K^{+}, Ona-soil Na^{+}, Ona-soil NO^{3-}, Oee-Electrochemical conductivity, Oph-soil pH, Osp-soil saturation percentage, Opo-soil phosphate.

Principle component analysis: The plant height was strongly associated with soil phosphate and soil NO^{3-} at large sand dunes of Cholistan (Fig. 5). The shoot length was strongly associated with soil Ca^{2+} and K^{+} at canal bank moist habitat. The fresh and dry weights of shoot were associated with soil Na^{+} and ECe at desert hypersaline flat of Cholistan (Fig. 5). Leaf epidermis thickness and cortical cell area were strongly associated with soil saturation percentage and soil Ca^{2+} at canal bank moist habitat. The hypodermis thickness and sclereid cell thickness were weakly associated with soil ECe and Na^{+} at desert saline flat of Cholistan and hypersaline flat of Cholistan (Fig. 5).

The hydrogen peroxide and soluble proteins related to soil Na^{+} and PO_4^{3-} at desert fenced area of Cholistan and desert plain of Thal (Fig. 5). The ascorbic acid, carotenoids and chlorophyll *b* were strongly associated with soil Na^{+} and soil ECe, whereas superoxide dismutase activity was linked to soil saturation percentage at desert saline flat of Cholistan and hypersaline flat of Cholistan. The glycine betaine, catalase and free amino acids coexisted with soil PO_4^{3-} and Ca^{2+} at large sand dunes of Cholistan and small sand dunes of Cholistan (Fig. 5). Physiological traits such as proline, chlorophyll *a*, soluble sugars, peroxidase and phenolics were associated with soil K^{+} at large sand dunes of Thal, desert flat of Cholistan, and canal bank moist habitat (Fig. 5).

Discussion

The overall response of structural and functional traits in *C. decidua* populations collected from hyperarid environments are summarized in Fig. 6. The populations of bare caper have modified morpho-anatomy and physiological characteristics regarding their habitats and soil physicochemical properties that permit them to survive in hyperarid and hot environments, which probably fixed in different population by exposure to a certain environmental condition for centuries. Several researchers proposed that the tolerant plant normally grows in heterogeneous environmental conditions (Marks *et al*., 2021; Stotz *et al*., 2021; Adams *et al*., 2023).

Bare caper populations were collected from different ecological habitats like canal banks, desert plains, desert small and large dunes, and desert saline and hypersaline flats. Plant height was better in large sand dunes population of Cholistan, which was linked to low soil saturation percentage and ECe. The sand dune habitats suited bare caper where it showed as also been stated by Hou *et al*., (2016). The moist habitat probably is not suitable for bare capers, which severely affected plant height. The saturation percentage, soil K^{+}, and soil Ca^{2+} were the highest at this habitat but this may not improve morphological traits, which is contradictory to the findings of Mbah (2012).

Capparis decidua is a tall shrub, but occasionally attains tree habits when growth of a plant is undisturbed (Singh & Singh, 2011). In the present study, all populations of this species attain shrubby growth, but canopy shape is different in different populations. The shoot length was increased in populations collected from small sand dunes, fenced areas, and desert flats of the Cholistan Desert, where soil ECe was low. This indicates a change in habits from bushy to elongated form, which is contradictory to most desert plants (Al-Tamimi & Al-Janabi, 2019). The hypersaline flat and saline flat populations of Cholistan showed the highest fresh and dry weights of shoots where soil Na^{+} and ECe were the maximum, this indicates high tolerance of bare caper to high salinity and hyperarid conditions (Peerzada & Naeem, 2018; Mansour *et al*., 2019).

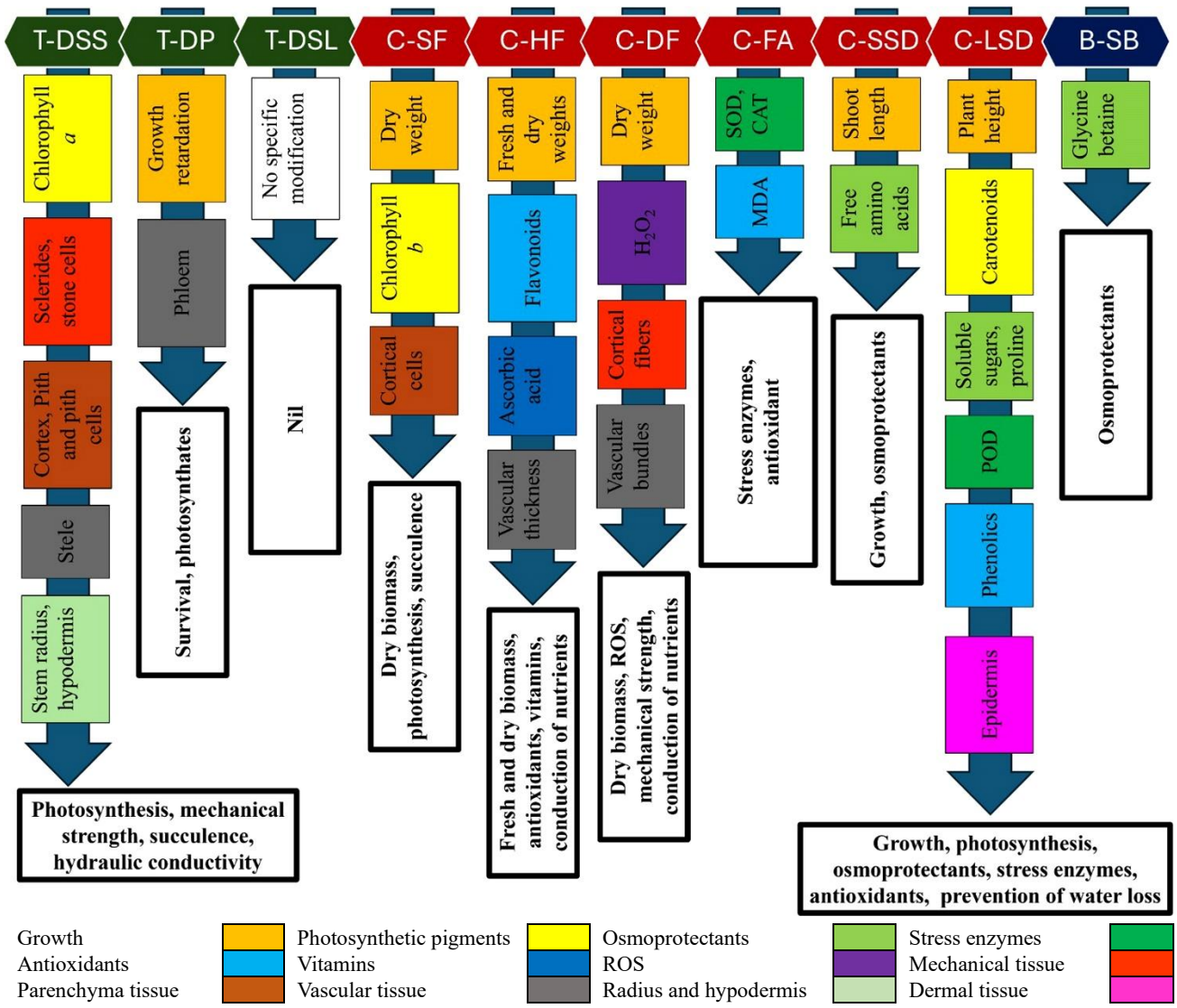

Fig. 6. Flowchart showing overall response of *Capparis decidua* populations collected from different hyperarid environments.

The bare caper had photosynthetic stem, in which hypodermis was with extensive sclerenchyma, aerenchyma, and chlorenchyma, as was reported by Dörken *et al*., (2020) in Australian *Tetratheca* and *Glischrocaryon* species. Among stem anatomical parameters, a huge variation recorded in stem radius, hypodermis thickness, cortical region thickness and its cell area, vascular bundle thickness and area, phloem thickness, pith cell thickness and stelar region thickness in all populations. Scleromorphy related traits such as collenchyma and sclereid cells in hypodermis, stone cells inside hypodermis, cortical fibers, and sclerification in the vascular region are of special importance. Such modifications are critically important under prolonged drought periods that limit water loss, provide mechanical support by preventing cell collapse and store water in photosynthetic tissue and storage parenchyma (Dörken *et al*., 2020). These stem parameters are essential in plants to enhance their succulence via pith parenchyma and prevent cell collapse via scleromorphic traits under stressful conditions (De Micco & Aronne, 2012).

Specialized cells such as sclereids, stone cells, and sclerenchyma fibers in hyperarid conditions protect metabolically active cells against solar radiation, repel herbivores, and reduce evapo-transpiration rate (Fortuna-Perez *et al*., 2021), as was observed in the populations from Thal-Small sand dunes, Thal-Large sand dunes, Cholistan-Small sand dunes, and Cholistan-Fenced area. Plants amplified the transport tissue by increasing vascularity through multiplying the number of broad metaxylem vessels (Naija *et al*., 2021). Enlarged metaxylem vessel area was observed in the populations from Cholistan-Desert flat and Cholistan-Saline flat. Access accumulation of Ca^{2+} may disturb physiological functions of a cell, hence preferably stored in parenchyma in the form of crystals (mostly calcium oxalate crystals) (He *et al*., 2024), as was recorded in the populations from Cholistan-Saline flat and Cholistan-Fenced area.

Another essential modification in bare caper to counteract water scarcity is the sunken stem stomata, which are clearly visible in the Cholistan-Fenced area population. Stomata in grooves can reduce transpiration rate significantly by protecting from direct exposure to external environments (e.g., strong winds and solar radiation) (Breckle & Rafiqpoor, 2022). The multifunctional hypodermis in bare caper is of special interest, which is composed of sclerenchyma,

parenchyma, chlorenchyma, and aerenchyma, but presence or absence of any tissue varied with collection sites. Multistratified hypodermis was also reported by Galviz & Valerio (2021) in *Jacquinia armillaris.* Extensive sclerification in epidermis and hypodermis was observed in the Thal-Small sand dunes population, which was covered by thick cuticle. Cuticle thickness works as a drought tolerance mechanism that not only limits water movement through plant surface, but also provides resistance to mechanical damage during hyperaridity (Bourgault *et al*., 2020). Sclerification in hypodermis is an adaptive feature that is critical for the maintenance of turgor of metabolically active tissue, and/or protect chlorenchyma from damage. Hypodermis essentially composed of sclerenchyma and chlorenchyma was noticed in the populations from Cholistan-Fenced area and Cholistan-Large sand dunes.

Most studies about water stress conditions indicated the reduction in stem radius and vascular bundle area likewise increase epidermis and sclerenchyma thickness (Naz *et al*., 2013; Quintana-Pulido *et al*., 2018; Bibi *et al*., 2022). In bare caper, the stem radius and cortical thickness increased in Thal-small sand dunes population, which is crucial for the enhanced water conservation capacity (i.e., succulence) in their parenchymatous cells (Wasim & Naz, 2020; Kandemir *et al*., 2020). This indicates bare caper more adaptable to hyperarid environmental conditions.

In bare caper, the main photosynthetic organ is stem (Liu *et al*., 2018). The desert populations showed low chlorophyll content, which is related to damage of the thylakoid membrane during stressful conditions (*Cicek et al*., 2018) in chickpea. Tolerant populations showed stable chlorophyll pigments that are adaptive features to environmental heterogeneity (Zhang *et al*., 2014).

All the populations from hyperarid habitats have more production in H_2O_2 molecules whereas populations from saline conditions have less ascorbic acid. All these enzymatic and non-enzymatic molecules are responsible for plant protection in hot and arid conditions of Thal and Cholistan (Kaya *et al*., 2018).

Conclusion

It is concluded that all the populations of *Capparis* showed exceptionally high variation in their morpho-anatomical and functional characteristics that play vital roles in maintaining water contents under hyperarid conditions. This is a strong reason for the broad distributional range of bare caper in diverse environmental conditions. Several traits are population specific that might develop independently in a specific set of environmental conditions. Scleromorphic traits such as lignin deposition in cortical, hypodermal region, and vascular bundles, stone cells, cortical fibers, and scleride cells were more developed in the Cholistan population with significantly higher dryness index. Plasticity in multisturctured hypodermis, which included chlorenchyma, sclerenchyma, parenchyma, and aerenchyma, is critically important for colonizing this species to extremely hot and hyperarid conditions.

Acknowledgement

This manuscript has been derived from Ph. D. Thesis of the first author submitted to University of Agriculture, Faisalabad.

References

Adams, W.W., J.J. Stewart, S.K. Polutchko, C.M. Cohu, O. Muller and B. Demmig-Adams. 2023. Foliar phenotypic plasticity reflects adaptation to environmental variability. *Plants*, 12: 2041.

Ahmad, K.S., M. Hameed, J. Deng, M. Ashraf, A. Hamid, F. Ahmad and N. Akhtar. 2016. Ecotypic adaptations in bermuda grass (*Cynodon dactylon*) for altitudinal stress tolerance. *Biologia*, 71. https://doi:10.1515/biolog-2016-0113

Akram, S., M. Ghaffar, A. Wadood, S. Shokat, A. Hameed, M.Q. Waheed and M.A.R. Arif. 2022. A GBS-based genome-wide association study reveals the genetic basis of salinity tolerance at the seedling stage in bread wheat (*Triticum aestivum* L.). *Front. Genet*., 13: 997901.

Alonso-Forn, D., D. Sancho-Knapik, J.P. Ferrio, J.J. Peguero-Pina, A. Bueno, Y. Onoda, J. Cavender-Bares, U. Niinemets, S. Jansen, M. Riedere, J.H.C. Cornelissen, Y. Chai and E. Gil-Pelegrín. 2020. Revisiting the functional basis of sclerophylly within the leaf economics spectrum of oaks: different roads to Rome. *Curr. For. Rep*., 6: 260-281.

Al-Tamimi, A.J. and A.S. Al-Janabi. 2019. Genetic diversity among bread wheat genotypes using RAPD and SSR markers. *SABRAO J. Breed. Genet*., 51: 325-339.

Arnon, D.I. 1949. Copper enzymes in isolated chloroplasts. Polyphenoloxidase in *Beta vulgaris*. *Plant Physiol*., 24: 1.

Bates, L.S., R.A. Waldren and I.D. Teare. 1973. Rapid determination of free proline for water-stress studies. *Plant Soil*, 39: 205-207.

Bibi, S., M.S.A. Ahmad, M. Hameed and A.K. Alvi. 2022. Modulation of physiological plasticity through structural and functional modifications in *Stipagrostis plumosa* L. for adaptability to hyper-arid environments. *Turk. J. Bot*., 46: 435-458.

Boughalleb, F., R. Abdellaoui, N. Ben-Brahim and M. Neffati. 2014. Anatomical adaptations of *Astragalus gombiformis* Pomel. under drought stress. *Open Life Sci.*, 9: 1215-1225.

Bourgault, R., S. Matschi, M. Vasquez, P. Qiao, A. Sonntag, C. Charlebois, M. Mohammadi, M.J. Scanlon, L.G. Smith and I. Molina. 2020. Constructing functional cuticles: analysis of relationships between cuticle lipid composition, ultrastructure and water barrier function in developing adult maize leaves. *Ann. Bot*., 125: 79-91.

Bradford, M.M. 1976. A rapid and sensitive method for the quantitation of microgram quantities of protein utilizing the principle of protein-dye binding. *Anal. Biochem*., 72: 248-254.

Breckle, S.W. and M.D. Rafiqpoor. 2022. Part J: ZB VII-Zonobiome of steppes and cold deserts or of arid temperate climate. In vegetation and climate. Berlin, Heidelberg, pp. 395-441.

Bremner, J.M. 1960. Determination of nitrogen in soil by the Kjeldahl method. *J. Agric. Sci*., 55: 11-33.

Budyko, M.I. 1961. The heat balance of the earth's surface. *Soviet Geog.,* 2: 3-13.

Chance, B. and A.C. Maehly. 1955. [136] Assay of catalases and peroxidases. 764-775.

Cheema, M.T., J.J. Ye, F.N. Li, Q.P. Lu, M. Abbas, I. Sajid, D.L. Huang, S.W. Liu and C.H. Sun. 2020. *Auraticoccus cholistanensis* sp. nov., an actinomycete isolated from soil of the Cholistan Desert and amended description of the genus *Auraticoccus. Int. J. Syst. Evol. Microbiol*., 70: 3179-3185.

Choat, B., S. Jansen, T.J. Brodribb, H. Cochard, S. Delzon, R. Bhaskar, S.J. Bucci, T.S. Feild, S.M. Gleason, U.G. Hacke and A.L. Jacobsen. 2012. Global convergence in the vulnerability of forests to drought. *Nature*, 491: 752-755.

Choat, B., T.J. Brodribb, C.R. Brodersen, R.A. Duursma, R. López and B.E. Medlyn. 2018. Triggers of tree mortality under drought. *Nature*, 558: 531-539.

Cicek, N., A. Oukarroum, R.J. Strasser and G. Schansker. 2018. Salt stress effects on the photosynthetic electron transport chain in two chickpea lines differing in their salt stress tolerance. *Photosyn. Res*., 136: 291-301.

Dahiya, R., J.S. Vaghela and R.K. Singh. 2019. A brief review on pharmacological and phytochemical studies of *Capparis decidua*. *Adv. Pharm. J*., 4: 133-139.

De Micco, V. and G. Aronne. 2012. Morpho-anatomical traits for plant adaptation to drought. In: Plant responses to drought stress. Springer, Berlin, Heidelberg, pp. 37-61.

Dhakad, P.K., P.K. Sharma and S. Kumar. 2016. A review on ethnobiological and medicinal potential of Capparaceae family plant: *Capparis decidua* (Forssk.) Edgew. *Adv. Pharm. Pharm. Sci*., 4: 27-39.

Ding, L., T. Milhiet, V. Couvreur, H. Nelissen, A. Meziane, B. Parent, S. Aesaert, M. Van Lijsebettens, D. Inzé, F. Tardieu and X. Draye. 2020. Modification of the expression of the aquaporin ZmPIP2; 5 affects water relations and plant growth. *Plant Physiol*., 182: 2154-2165.

Dörken, V.M., P.G. Ladd and R.F. Parsons. 2020. Anatomical aspects of xeromorphy in arid-adapted plants of Australia. *Aust. J. Bot*., 68: 245-266.

Fortuna-Perez, A.P., C.R. Marinho, M. Vatanparast, W. de Vargas, J.R.V. Iganci, G.P. Lewis, E.S. Candido, T.M. de Moura, T.C. de Monteiro, S.T.S. Miotto and S.P. Teixeira. 2021. Secretory structures of the *Adesmia clade* (Leguminosae): implications for evolutionary adaptation in dry environments. *Perspect Plant Ecol. Evol. Syst*., 48: 125588.

Gadiwala, M.S., F. Burke, M.T. Alam, S. Nawaz-ul-Huda and M. Azam. 2013. Oceanite and continentality climate indices in Pakistan. *Malays. J. Soc. Space*, 9: 57-66.

Galviz, Y.C. and R. Valerio. 2021. Leaf morphoanatomical traits of *Jacquinia armillaris* Jacq. (Theophrastoideae-Primulaceae) in two xeric shrublands from Venezuela. *Neotrop. Biodiv.*, 7: 364-375.

Giannopolitis, C.N. and S.K. Ries. 1977. Superoxide dismutases: I. Occurrence in higher plants. *Plant Physiol*., 59: 309-314.

Grieve, C.M. and S.R. Grattan. 1983. Rapid assay for determination of water-soluble quaternary ammonium compounds. *Plant Soil*., 70: 303-307.

He, H., D. Li, X. Li and L. Fu. 2024. Research progress on the formation, function, and impact of calcium oxalate crystals in plants. *Crystallogr. Rev*., 1-30.

Heath, R.L. and L. Packer. 1968. Photoperoxidation in isolated chloroplasts: II. Role of electron transfer. *Arch. Biochem. Biophys*., 125: 850-857.

Hou, Q., G. Ufer and D. Bartels. 2016. Lipid signaling in plant responses to abiotic stress. *Plant Cell Environ*., 39: 1029-1048.

Ivanova, L.A., P.K. Yudina, D.A. Ronzhina, L.A. Ivanov and N. Hölzel. 2018. Quantitative mesophyll parameters rather than whole-leaf traits predict response of C3 steppe plants to aridity. *New Phytol*., 217: 558-570.

Jackson, M.L. 1962. Interlayering of expansible layer silicates in soils by chemical weathering. *Clays Clay Miner*., 11: 29-46.

Julkunen-Tiitto, R. 1985. Phenolic constituents in the leaves of northern willows: methods for the analysis of certain phenolics. *J. Agric. Food Chem*., 33: 213-217.

Kandemir, N., A. Çelik, S.N. Shah and A. Razzaq. 2020. Comparative micro-anatomical investigation of genus *Heliotropium* (Boraginaceae) found in Turkey. *Flora*, 262: 151495.

Kaya, C., A.A. Akram, M. Ashraf and O. Sonmez. 2018. Exogenous application of humic acid mitigates salinity stress in maize (*Zea mays* L.) plants by improving some key physico-biochemical attributes. *Cereal Res. Comm.*, 46: 67-78.

Kumar, D.S., A. Shukla, P.K. Choudhury and G.K. Singh. 2015. Analgesic and anti-nociceptive activity of hydroethanolic extract of *Capparis decidua* Linn. *Asian J. Pharm. Pharmacol*., 1: 40-44.

Lettau, H. 1969. Evapotranspiration climatonomy: I. A new approach to numerical prediction of monthly evapotranspiration, runoff, and soil moisture storage. *Mon. Weather Rev*., 97: 691-699.

Liu, J., L. Gu, Y. Yu, G. Ju and Z. Sun. 2018. Stem photosynthesis of twig and its contribution to new organ development in cutting seedlings of *Salix matsudana* Koidz. *Forests*, 9: 207.

Mansoor, U., S. Fatima, M. Hameed, M. Naseer, M.S.A. Ahmad, M. Ashraf and M. Waseem. 2019. Structural modifications for drought tolerance in stem and leaves of *Cenchrus ciliaris* L. ecotypes from the Cholistan Desert. *Flora*, 261: 151485.

Mansour, H.A., S.K. Abd-Elmabod and B.A. Engel. 2019. Adaptation of modeling to the irrigation system and water management for corn growth and yield. *Plant Arch*., 19: 644-651.

Marks, R.A., J.M. Farrant, D. Nicholas McLetchie and R. VanBuren. 2021. Unexplored dimensions of variability in vegetative desiccation tolerance. *Am. J. Bot*., 108: 346-358.

Mbah, C.N. 2012. Determining the field capacity, wilting point and available water capacity of some Southeast Nigerian soils using soil saturation from capillary rise. *Niger. J. Biotechnol*., 24: 41-47.

Mir, S., M. Ahmad, M.A. Khan, M. Zafar, S. Jahan, S. Sultana and S. Majeed. 2019. Palyno-morphological investigations of subtropical endangered flora of Capparidaceae through light and scanning electron microscopy. *Microsc. Res. Tech*., 82: 1401-1409.

Moore, S. and W.H. Stein. 1948. Photometric ninhydrin method for use in the chromatography of amino acids. *J. Biol. Chem*., 176: 367-388.

Mukherjee, S.P. and M.A. Choudhuri. 1983. Implications of water stress-induced changes in the levels of endogenous ascorbic acid and hydrogen peroxide in *Vigna* seedlings. *Physiol. Plant*, 58: 166-170.

Naija, D.S., S.B.M. Gueddes and M. Braham. 2021. Effects of water scarcity and salinity on the anatomy of the Tunisian table olive cultivar 'Meski'. *Not. Bot. Horti. Agrobo. Cluj-Napoca*., 49: 12157.

Naz, N., M. Hameed, T. Nawaz, R. Batool, M. Ashraf, F. Ahmad and T. Ruby. 2013. Structural adaptations in the desert halophyte *Aeluropus lagopoides* (Linn.) Trin. ex Thw. under high salinity. *J. Biol. Res*., 19: 150-164.

Oliveira, I., A. Meyer, S. Afonso and B. Gonçalves. 2018. Compared leaf anatomy and water relations of commercial and traditional *Prunus dulcis* (Mill.) cultivars under rain-fed conditions. *Sci. Horti.,* 229: 226-232.

Onsa, G.H., N. bin Saari, J. Selamat and J. Bakar. 2004. Purification and characterization of membrane-bound peroxidases from *Metroxylon sagu*. *Food Chem*., 85: 365-376.

Palta, J.A., J.D. Berger and H. Bramley. 2012. Physiology of the yield under drought: Lessons from studies with lupin. In: Plant responses to drought stress. Springer, Berlin, Heidelberg, pp. 417-440.

Pan, T., M. Liu, V.D. Kreslavski, S.K. Zharmukhamedov, C. Nie, M. Yu, V.V. Kuznetsov, S.I. Allakhverdiev and S. Shabala. 2020. Nonstomatal limitation of photosynthesis by soil salinity. *Crit. Rev. Environ. Sci. Technol*., 51: 1-35.

Patil, M.P. and C.V. Murumkar. 2017. Occurrence of CAM activity in stem of *Capparis decidua* (Forssk.) Edgew. *Genet. Plant Physiol*., 7: 171-17.

Peerzada, A.M. and M. Naeem. 2018. Germination ecology of *Cenchrus biflorus* Roxb.: Effects of environmental factors on seed germination. *Rangel. Ecol. Manag*., 71: 424-432.

Quintana-Pulido, C., L. Villalobos-González, M. Muñoz, N. Franck and C. Pastenes. 2018. Xylem structure and function in three grapevine varieties. *Chilean J. Agric. Res*., 78: 419-428.

Quiroga, R.E., A.C. Premoli and R.J. Fernández. 2021. Niche dynamics in amphitropical desert disjunct plants: Seeking for ecological and species-specific influences. *Glob. Ecol. Biogeogr*., 30: 370-383.

Rady, M.M., W.M. Semida, K.A. Hemida and M.T. Abdelhamid. 2016. The effect of compost on growth and yield of *Phaseolus vulgaris* plants grown under saline soil. *Int. J. Recycl. Org. Waste Agric*., 5: 311-321.

Rafay, M., M. Madnee, M.I. Ashraf, M. Abid, M.U. Ghaffar, Z. Malik, H. Basit and S.U. Hassan. 2022. Phytoremediation capabilities and antioxidant enzymes'activities of two halophytic shrubs *Capparis decidua* and *Haloxylon salicornicum* from Cholistan desert, Pakistan under salinity stress. *Pak. J. Bot*., 54: 1231-1236.

Rouphael, Y., V. De Micco, C. Arena, G. Raimondi, G. Collaand and S. De Pascale. 2017. Effect of *Ecklonia maxima* seaweed extract on yield, mineral composition, gas exchange, and leaf anatomy of *Zucchini* squash grown under saline conditions. *J. Appl. Phycol*., 29: 459-470.

Sharif. F. and A.U. Khan. 2009. Alleviation of salinity tolerance by fertilization in four thorn forest species for the reclamation of salt-affected sites. *Pak. J. Bot*., 41: 2901-2915.

Singh, D. and R.K. Singh. 2011. Kair (*Capparis decidua*): A potential ethnobotanical weather predictor and livelihood security shrub of the arid zone of Rajasthan and Gujarat. *Ind. J. Trad. Know*., 10: 146-155.

Stotz, G.C., C. Salgado-Luarte, V.M. Escobedo, F. Valladares and E. Gianoli. 2021. Global trends in phenotypic plasticity of plants. *Ecol. Lett*., 24: 2267-2281.

Tesfaye, M. and M. Negash. 2018. *Combretum-Terminalia* vegetation accumulates more carbon stocks in the soil than the biomass along the elevation ranges of dryland ecosystem in Southern Ethiopia. *J. Arid Environ*., 155: 59-64.

Toth, S.J. and A.L. Prince. 1949. Estimation of cation-exchange capacity and exchangeable Ca, K, and Na contents of soils by flame photometer techniques. *Soil Sci*., 67: 439-446.

Tripathi, D.K., V.P. Singh, S.M. Prasad, D.K. Chauhan and N.K. Dubey. 2015. Silicon nanoparticles (SiNp) alleviate chromium (VI) phytotoxicity in *Pisum sativum* (L.) seedlings. *Plant Physiol. Biochem*., 96: 189-198.

UNESCO. 1979. Map of the world distribution of arid regions-explanatory notes. MAB technical notes 7. United nations educational, Scientific and cultural organization, Paris.

Velikova, V., I. Yordanov and A.J.P.S. Edreva. 2000. Oxidative stress and some antioxidant systems in acid rain-treated bean plants: protective role of exogenous polyamines. *Plant Sci*., 151: 59-66.

Verma, P.D., R. Dangar, R. Dangar and B. Suhagia. 2012. A pharmacognostical study on stem of *Capparis decidua* Edgew. *Int. J. Pharm. Res. Technol*., 2: 28-32.

Vyas, P. and A Gulati. 2009. Organic acid production *In vitro* and plant growth promotion in maize under controlled environment by phosphate-solubilizing fluorescent Pseudomonas. *B.M.C. Microbiol*., 9: 1-15.

Wang, Y.X., R.M. Teng, W.L. Wang, Y. Wang, W. Shen and J. Zhuang. 2019. Identification of genes revealed differential expression profiles and lignin accumulation during leaf and stem development in tea plant (*Camellia sinensis* (L.) O. Kuntze). *Protoplasma*, 256: 359-370.

Wasim, M.A. and N. Naz. 2020. Anatomical adaptations of tolerance to salt stress in *Cenchrus ciliaris* L., a saline desert grass. *J. Anim. Plant Sci*., 30: 1548-1566.

Wolf, B. 1943. Rapid determination of soluble nutrients in soil and plant extracts by means of photelectric colorimeter. *Ind. Eng. Chem. Anal. Ed*., 15: 248-251.

Yemm, E.W. and A. Willis. 1954. The estimation of carbohydrates in plant extracts by anthrone. *Biochem. J*., 57: 508.

Zhang, Y., G.H. Xia, K. Ma, G.Y. Li, Y.C. Dai and C.X. Yan. 2014. Effects of shade on photosynthetic characteristics and chlorophyll fluorescence of *Ardisia violacea*. *Chin. J. Appl. Ecol*., 25: 1940-1948.

Zhishen, J., T. Mengcheng and W. Jianming. 1999. The determination of flavonoid contents in mulberry and their scavenging effects on superoxide radicals. *Food Chem*., 64: 555-559.

(Received for publication 15 June 2024)